

# Design-Informatics Approach for Intimate Configuration of Silent Supersonic Technology Demonstrator

Kazuhisa Chiba\*, Yoshikazu Makino† and Takeshi Takatoya‡  
*Japan Aerospace Exploration Agency, Tokyo 182-8522, Japan*

The *design-informatics approach* has been suggested for the efficient design. In the present study, this approach was applied to the design for the intimate configuration of the silent supersonic technology demonstrator. The design-informatics approach has two steps such as optimization and data mining. As a present first step, multidisciplinary design optimization with multi-objectives was performed among aerodynamics, structures, aeroelasticity, and boom noise. The optimization problem had four objective functions as the minimizations of the pressure drag and the boom intensity at supersonic condition, and the structural weight of wing made from composite and aluminum materials as well as the improvement of the trim performance. The intimate configuration was optimized on the hybrid method between the particle swarm optimization and genetic algorithm. As a present second step, data mining was carried out by using the self-organizing map and the analysis of variance to extract the design knowledge from the acquired optimization results for deciding a conclusive compromise solution. Consequently, a compromise solution was successfully determined because all the designers could specifically share the beneficial design information. The design-informatics approach is essential for an efficient design process.

## I. Introduction

DESIGN-INFORMATICS approach composed by optimization and data mining is the efficient design manner. Especially, it is effective to the design of aerospace vehicle which is a large-scale problem and has the evaluations with troubles for many design requirements. The word as large scale mentioned here has two senses as follows. a) the huge time to evaluate objective functions in high-fidelity is needed. b) the many design variables are necessary for the definition of an intimate configuration. When the large-scale problem as a) is considered, approximation methods typified as a response surface method can resolve it. However, when the large-scale problem as b) is considered, it is difficult to manage that problem. Therefore, heuristic algorithms typified as evolutionary algorithms should be selected for the optimization problems with a large number of design variables. One of the reasons is that heuristic algorithms can efficiently explore large design space with independence of objective functions. Another reason is that each design objective should be managed as independent objective functions to obtain tradeoff information (Pareto solutions) in multiobjective optimization problem. So, heuristic algorithms should be employed for a large-scale optimization problem. But, sufficiently evolved solutions are not achieved due to the time restraint. In the case of the present study, it took roughly seven days at least for one generation. As the order of the fourth power of 10 at least is necessary for sufficient evolution in the information science, it should take 20 years for the present optimization. This number is impractical. Consequently, even when an optimization is performed by using maximum period as much as possible, it is difficult to acquire the solution with which designers are satisfied from its result. Thus, the operation as data mining is carried out for the set of solutions obtained by an optimization. Since, this operation stipulates the design information existed in design space, a desirable final compromise solution would be conducted from an optimization result. The design information is as follows; 1) tradeoffs among objective functions, 2) correlations between objective

---

\*Project Researcher, Aviation Program Group; currently Lecturer, Hokkaido Institute of Technology. Member AIAA.

†Senior Researcher, Aviation Program Group. Member AIAA.

‡Senior Researcher, Aviation Program Group.

Copyright © 2009 by the American Institute of Aeronautics and Astronautics, Inc. All rights reserved.

functions and design variables, 3) experience and scent considered unconsciously during the definition of an optimization problem, 4) the flaw in the definition of an optimization problem. In addition, as the design information would have the knowledge that designers never consider, it would yield the seed for an innovative design. This study denominates the present methods between the optimization for a large-scale problem and data mining the design informatics approach, and then the systematic management would be proposed. In addition, this approach is applied for the silent supersonic technology demonstrator (S3TD)<sup>1</sup> so that a compromise solution is determined.

Since the flight experiment of the non-powered supersonic experimental scaled airplane NEXST-1 was succeeded in October 2005<sup>2</sup>, S<sup>3</sup>TD then has been researching and developing as a next step in Japan Aerospace Exploration Agency (JAXA). In the previous work, the 2nd shape was redesigned<sup>3</sup>. The purpose of the previous work was the decision of the main wing planform using the multidisciplinary design exploration. The design requirements included the lift, friction drag. The structural requirements were defined by the strength and vibration of the main wing. In addition, the design configuration was simply wing-fuselage configuration. On the other hand, the purpose of the present study is the design of the three-dimensional main wing and the security of the body stability and the 3rd shape is updated. The design requirements do not investigate the lift and the friction drag due to the fixed planform shape but add the stability. The structural requirements are defined by the strength and flutter of the main wing. Moreover, the design configuration is strictly an intimate configuration constructed as the main wing, fuselage, vertical tail wing, stabilizer, and engine system to evaluate the trim performance and accurate rear boom intensity.

By the way, multidisciplinary design optimization (MDO) is essential for practical engineering designs. However, as a multi-objective (MO) problem has generally tradeoffs as an optimum set (it is called as Pareto-optimal solutions or non-dominated solutions), an MO optimization should be performed to identify such tradeoffs and correlations efficiently. MO evolutionary algorithms (MOEAs) were applied to MO optimizations to sample multiple non-dominated solutions because evolutionary algorithms (EAs) sought optimum solutions in parallel using a population of design candidates. In this study, the hybrid method between MO particle swarm optimization (PSO) and adaptive range MOGA<sup>4</sup> was applied to search both global and local optimum solutions efficiently. Moreover, the design information acquired from MO optimization result by performing data mining is necessary for the decision making of a compromise design. The result of MDO afresh has the meaning to obtain the design information using data mining.

The objective of the present study is to design the 3rd intimate-configuration shape of the S<sup>3</sup>TD using the design-informatics approach, *i.e.*, to optimize the airfoil shapes of main wing which the planform is fixed and the deflection angle of the stabilizer for the intimate configuration of the S<sup>3</sup>TD using computational fluid dynamics and computational structural dynamics evaluation tools, on a PSO/GA hybrid method. Moreover, the design information for S<sup>3</sup>TD is extracted from the optimization result by using data mining, a compromise solution is then determined through the designers' discussion using the design knowledge.

## II. Design-Informatics Approach

Figure 1 shows the flowchart of the present design-informatics approach. The design problem was firstly defined such as objective functions, constraints, and design space. And then, optimization was performed to obtain non-dominated solutions for database construction. When non-dominated solutions are lopsidedly in design space, response surface method is frequently used to uniform the location of solutions. In this study, the obtained non-dominated solutions were directly employed as the design database. For generated design database, data mining was performed to extract useful design knowledge such as tradeoffs and the correlation among the objective functions, the characteristic performances, and the design variables. Of course, not only non-dominated solutions but also all solutions can be employed as database, but non-dominated solutions are used in this study to efficiently select a beneficial compromise solution. In addition, it is confirmed that the design knowledge obtained from non-dominated solutions is connoted that acquired from all solutions<sup>5</sup>.

### A. Multidisciplinary Design Optimization

The present MDO is performed among aerodynamics, structures, aeroelasticity, and boom noise. An intimate configuration of the 2.5th latest shape composed by main wing, fuselage, vertical tail wing, stabilizer, and engine system is considered as shown in Fig. 2 to strictly evaluate each objective. It is notable that the 2.5th shape had the main wing whose cross section was defined as a symmetrical airfoil. Since the aerodynamic

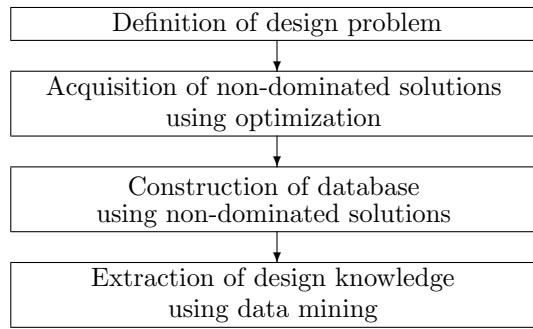


**Figure 1. Flowchart of the design-informatics approach.**

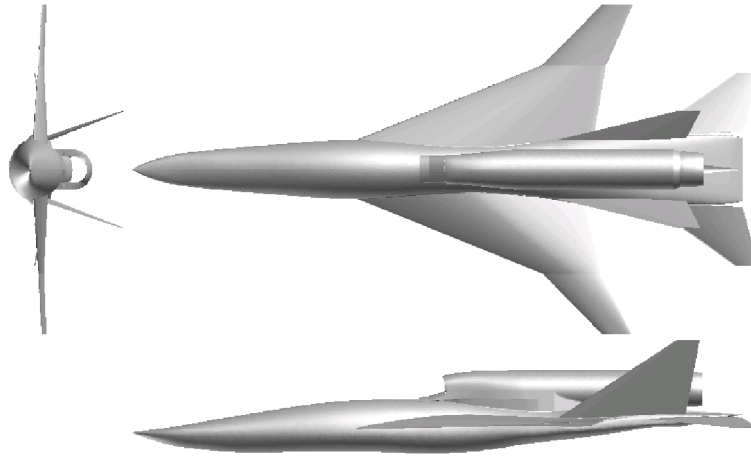


**Figure 2. Three views for the intimate configuration of 2.5th shape.**

performance of this geometry was strictly evaluated by using a Navier-Stokes computation on structured mesh in another study, the evaluation manner in the present optimization is different. Therefore, the performances between the 2.5th shape and the present optimization results are not necessarily compared. In addition, as the 2.5th shape did not trim, the geometry design to trim is the primary objective of this optimization. The optimization target is airfoil shapes of the main wing cross section at root, kink, and tip positions, and the deflection angle of the stabilizer. The flowchart of the MDO system is shown in Fig. 3.

### 1. Objective Functions

1. The minimization of the pressure drag  $C_{D_p}$  at the supersonic cruising condition, which is defined as Mach number of 1.6, altitude of 14km, and target  $C_L$  of 0.055. The target  $C_L$  is constant due to the fixed planform.
2. The minimization of the intensity of sonic boom  $I_{boom}$  at the supersonic cruising condition. This objective function value is defined as  $|\Delta P_{max}| + |\Delta P_{min}|$  at the location with largest (smallest) peak of sonic-boom signature across boom carpet.
3. The minimization of structural weight  $W$  for a main wing. The inboard and outboard wings are respectively defined as metal and composite materials. The minimum wing weight is solved with the fulfillment of the strength and flutter requirements. For the inboard wing made of metal, the thicknesses of skin and multi-frames are optimized. In addition, for the outboard wing made of composite material, the stacking sequence is optimized. These are the combination optimizations, and these are the nesting constitution for the present MDO.

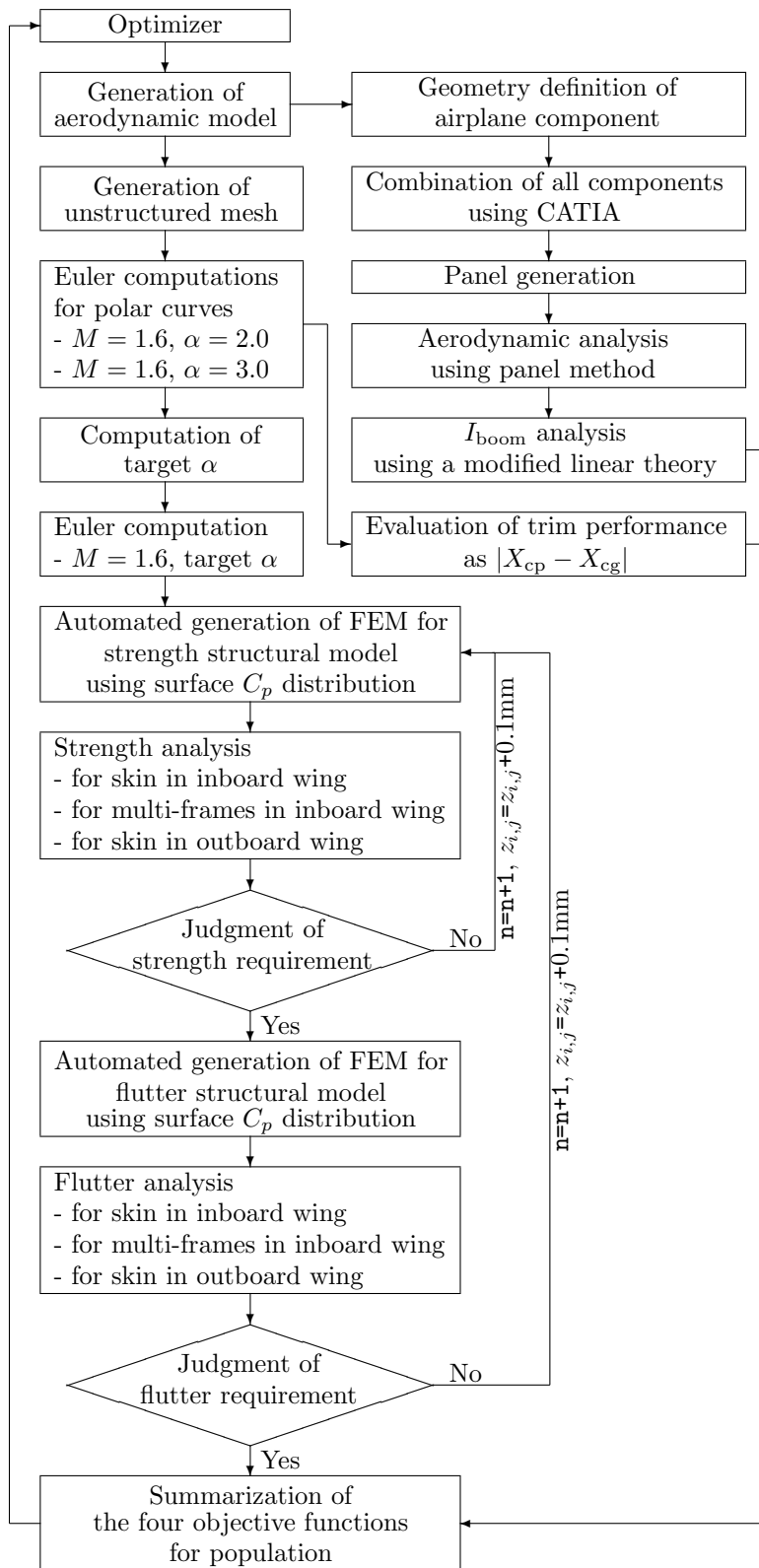


Figure 3. Flowchart of the present multidisciplinary design optimization part.  $n$  denotes the number of the symmetrical stacking of laminated composites on the outboard wing.  $z_{i,j}$  are each thickness of the skin and multi-frames in inboard wing

4. The minimization of the difference between the centers of pressure and of gravity  $|x_{cp} - x_{cg}|$  to trim. It is notable that MAC denotes mean aerodynamic chord. The center of pressure is calculated as follows.

$$\begin{aligned} x_{cp} &= x_{ref} - \frac{C_{Mp}}{\text{target}C_L} \times \text{MAC} \\ x_{ref} &= 25\% \text{MAC} \end{aligned} \quad (1)$$

On the other hand, the center of gravity  $x_{cg}$  is computed from the aerodynamic center  $N_0$  as follows.

$$\begin{aligned} x_{cg} &= N_0 - \text{const.} \\ &= x_{ref} - \frac{\Delta C_{Mp}}{\Delta C_L} \times \text{MAC} - \text{const.} \end{aligned} \quad (2)$$

where, the constant value *const.* in eq.(2) is defined by the results of Navier-Stokes computations in advance. It is set on 0.817[m] in this study.

## 2. Geometry Definition

The planform of the main wing and the configurations of the fuselage, the engine, the vertical tail wing, and stabilizer are fixed. The design variables are related to the airfoil shapes, the twist, the position relative to the fixed fuselage for the main wing as well as the deflection angle of the stabilizer. Airfoil shapes are defined at the root, kink, and tip of the main wing by using distribution of the thickness and the camber line. The thickness distribution is described by Bézier curve using nine control points (10 design variables), and linearly interpolated in the spanwise direction. The camber line is parameterized by using Bézier curves with four control points (four design variables), and incorporated linearly in the spanwise direction. The wing twist is represented by B-spline curve using six control points (six design variables). The twist center is defined at 80% chordwise position so that the straight hinge line for aileron is secured. The position of the wing root relative to the fuselage is parameterized by  $z$  coordinate (heightwise direction) of the leading edge, angle of attack, and dihedral. That is, the wing position of the chordwise direction relative to the fuselage is fixed. The entire computational aerodynamic geometry was thus defined by 50 design variables. The detail of the design variables is summarized in Table 1. The serial number in Table 1 is employed in the optimizer.

On the other hand, a structural geometry does not have one-to-one correspondence for an aerodynamic geometry. A structural geometry is uniquely determined by the objective function as the minimization of the main-wing weight  $W$  for an aerodynamic geometry. In the present study, the main wing separates the inboard and outboard wings using the threshold of the maximum wing thickness. The maximum wing thicknesses at each spanwise location are measured from the root. When it becomes less than 50 [mm], the spanwise region from the root to that position is defined as the inboard wing. The outer spanwise region from that position is defined as the outboard wing. The inboard wing is compounded as multi-frame structure made from aluminum material. It is described by two design variables such as the thicknesses of the skin and the multi frames. The outboard wing is composed as full-depth honeycomb sandwich structure made from a composite material defined as symmetrical stacking  $[0/\theta/-\theta/90]_{ns}$ .  $\theta$  is set as 15, 30, 45, 60, and 75deg. Whenever only one fiber angle is fulfilled for the structural requirements, the individual is judged to be satisfied with them. It is described by two design variables such as the fiber angle of a ply  $\theta$  and the number of symmetrical stacking  $n$  ( $n$  corresponds to  $\mathbf{n}$  used in Fig. 3). Hence, the total number of four design variables is used to describe the wing structural geometry. Note that these four design variables is subsidiary to 50 design variables for the aerodynamic geometry.

## 3. Optimizer

A hybrid method<sup>4</sup> between MOPSO<sup>6,7</sup> and the adaptive range MOGA(ARMOGA)<sup>8,9</sup> is employed. Recent optimization work often uses a response surface model(RSM) based on the Kriging statistical model to restrain evaluation time<sup>10-12</sup>. However, when the optimization problem with many design variables is considered, the many initial sample points are needed to maintain the accuracy of response surface<sup>13</sup>. In the present study, RSM is not selected to avoid a large evaluation time for many initial samples because they are merely individuals generated at random in design space. In addition, since the designers required to present many optimum solutions for the decision of a compromise one, an evolutionary-based Pareto approach as an efficient multi-thread algorithm was employed instead of gradient-based method.

**Table 1. Detail of design variables. The serial number of 1 to 49 is set for the main wing, and the serial number of 50 is set for the stabilizer.**

<i>serial number</i>	<i>correspondent design variable</i>	
1	$z$ coordinate	at root leading edge
2	cant angle for attachment to fuselage	
3	dihedral angle	
4 - 15	control points for camber	root, kink, tip
16 - 45	control points for thickness	root, kink, tip
46 - 49	control points for twisting angle	47 is set at kink
50	reflection angle of stabilizer	

GAs have generally not for a capability to search local optima but for a faculty of global search. On the other hand, PSO is efficient to search for local optima because it deals with the coordinates of design variables directly. The hybridization between them would produce both capabilities. As PSO and GA use mutation (called as perturbation in PSO) for the maintenance of solution diversity and the prevention of convergence to a local optima, the convergence to Pareto solutions becomes worse. The PSO/GA hybrid method improves of diversity and enriches the quality of the obtained solutions.

The real-coded MOGA is used in this study because the value of design variables is directly employed for the chromosome of individual. Regarding crossover, the blended crossover method (BLX- $\alpha$ )<sup>14</sup>, and the principal component analysis-BLX- $\alpha$  method (PCA-BLX- $\alpha$ )<sup>15</sup> are employed, and then the quarter of the population size is assigned to each crossover method. The other population was assigned to PSO. When the mutation rate is high, an EA search is close to a random search and results in slow convergence. Therefore, the mutation rate is defined by using the inverse of the number of design variable.

#### 4. Constraints

The several geometrical constraints are considered as follows. The planform of the main wing is fixed. The maximum thickness of the main wing at root and kink has limit from 4% to 6% chord length. The maximum thickness at tip has also limit from 2% to 4% chord length. The camber line of the main wing does not wave at root, kink, and tip. That is, a wavy surface wing is not considered. The twisting angle of the main wing is monotonously reduced at spanwise. The control point for twisting angle exists at kink. The generated main wing stays in the fuselage. The number of the symmetrical stacking  $n$  is set on  $\forall n \in \mathbf{N} \leq 25$ . When  $n$  is greater than 25, the individual is not judged to be able to fulfill the structural requirements. Therefore, a rank has penalty in the optimizer.

#### 5. Evaluation Method

The present optimization system provides three evaluation modules for aerodynamics, structures, and boom noise. As the structures module uses the result of aerodynamic evaluation, these phases are carried out one by one. The master processing element (PE) manages PSO/GA, while the slave PEs computed those three evaluation processes. Slave processes do not have to synchronize. It takes roughly seven days at least to evaluate one generation using 400CPUs of the Central Numerical Simulation System (CeNSS) of Numerical Simulator III in JAXA. It is notable that the accuracy of each evaluation tool for aerodynamics, structures, and boom noise was validated through NEXST-1 design<sup>16,17</sup> and the conceptual design for S<sup>3</sup>TD 2nd configuration<sup>18</sup>.

##### 5.1 Aerodynamic Evaluation

In the present study, TAS-Code, parallelized unstructured Euler/Navier-Stokes solver using domain decompositions and message-passing interface (MPI) library, is employed. The three-dimensional Euler equations are solved with a finite-volume cell-vertex scheme on the unstructured mesh<sup>19</sup>. The Harten-Lax-van Leer-Einfeldt-Wada Riemann solver<sup>20</sup> is used for the numerical flux computations. The Venkatakrishnan's limiter<sup>21</sup> is applied when reconstructing the second order accuracy. The lower-upper symmetric-Gauss-Seidel

implicit scheme<sup>22</sup> is applied for time integration.

Euler computations are performed under subsonic and supersonic flight conditions, respectively. Taking advantage of the parallel search in PSO/GA, the present optimization is parallelized. Moreover, the aerodynamic computation is also parallelized on the scalar machine.

### 5.2 Structural Evaluation

In the present MDO system, structural optimization of the thickness of each multi-frame for inboard wing and the stacking sequence optimization of laminated composites for outboard wing are simultaneously performed to realize minimum  $W$  fulfilling the constraints of strength and flutter requirements. Given the wing outer mold line for each individual, finite element model (FEM) is automatically generated from aerodynamic evaluation result of supersonic cruising condition, such as coordinates, pressure coefficient, and normal vector ( $x$ ,  $y$ ,  $z$ ,  $C_p$ ,  $x_\perp$ ,  $y_\perp$ , and  $z_\perp$ ). The strength and flutter characteristics are evaluated by using the commercial software MSC. NASTRAN<sup>TM</sup>.

First, the strength analysis is carried out until four design variables fulfill the strength requirement at each node of FEM mesh on each laminated composite. The strength requirement is defined that the criteria for composite is less than 1.0 and also von Mises stress is less than 200[MPa]. Then, the flutter analysis is performed to set the combinations of the design variables satisfied with the strength requirement until they fulfill the flutter requirements. The flutter requirement is defined that the flutter speed is greater than 462m/sEAS for the all conditions of Mach number of 0.85, 0.80, 0.95, and 0.98. Flutter speed is perceived by using U-g method. This flutter limitation is defined from the grade for NEXST-1<sup>2</sup>. It is notable that the flutter analysis is performed for only main wing. The full flutter analysis for the intimate configuration would be performed in the detailed design phase. The computational condition is set on the symmetrical maneuver +6G and the margin of safety is set on 1.25. The speed of sound and the air density are set under the condition of altitude of 14km.

### 5.3 Sonic Boom Evaluation

The computer-aided design(CAD)-based Automatic Panel Analysis System (CAPAS)<sup>18</sup> is used to evaluate  $I_{boom}$ . CAPAS is a conceptual aerodynamic design tool in JAXA. This tool comprised four design processes as follows; 1) geometry definition of airplane component, 2) combination of all components in an airplane configuration using an application program interface for the CATIA<sup>TM</sup>V4, 3) generation of panel and aerodynamic analysis using panel method, 4) sonic-boom analysis using a modified linear theory. As an aerodynamic evaluation module in CAPAS is low-fidelity because a geometry is inaccurate due to rough computational panel, the aerodynamic performance in CAPAS is used only to evaluate  $I_{boom}$ .

## B. Data Mining

Although a design optimization is important for engineering, the most significant point is the extraction of the knowledge in design space. The results obtained by MO optimization are not a sole solution but an optimum set. That is, as multi-objective optimization result is insufficient information for practical design because designers need a conclusive shape. However, the result of MO optimization can be accounted as a hypothetical design database. Data mining as a post-process for an optimization is essential to obtain the fruitful design knowledge efficiently<sup>23,24</sup>. That is, MO optimization and data mining should be unify to handle as an efficient design manner. A sequence of systemized system would be called as design-informatics approach. In the present study, functional analysis of variance<sup>25,26</sup> (ANOVA) and self-organizing map<sup>27</sup> (SOM) are used as the data mining technique. The distinguishing feature of a self-organizing map is the generation of a qualitative description. The advantage of this method includes the intuitive visualization of two-dimensional colored maps of design space using bird-eye-like views. As a result, SOM directly reveals the tradeoffs among objective functions. Moreover, SOMs roughly address the effective design variables and also reveal how a specific design variable affects objective functions and other design characteristics. However, SOM is subjective due to color cognizance. There is also a possibility of oversight because of a large number of objective functions and design variables. On the other hand, the distinguishing property of ANOVA is the quantitative description. The advantage of this method is the fact that it directly finds globally effective design variables. But, ANOVA cannot directly identify the effects of design variables on objective functions. When two methods are combined together, the results obtained can compensate with the disadvantages of the individual methods<sup>5</sup>.

ANOVA is one of the data mining techniques showing the effect of each design variable to the objective and the constraint functions in a quantitative manner. ANOVA uses the variance of the model due to the design variables on the approximation function. By decomposing the total variance of model into the variance due to each design variable, the influence of each design variable on the objective function can be calculated. The decomposition is accomplished by integrating out the variables of model  $\hat{f}$ .  $\hat{f}$  denotes an estimated value of unknown function  $f$ .

On the other hand, SOM is an unsupervised learning, nonlinear projection algorithm from high to low-dimensional space. This projection is based on self-organization of a low-dimensional array of neurons. In the projection algorithm, the weights between the input vector and the array of neurons are adjusted to represent features of the high dimensional data on the low-dimensional map. The close two patterns are in the original space, the closer is the response of two neighboring neurons in the low-dimensional space. Thus, SOM reduces the dimension of input data while preserving their features. The standard Kohonen algorithm adjusts the weight vector after all each record is read and matched. On the contrary, the Batch-SOM takes a ‘batch’ of data (typically all records), and performs a ‘collected’ adjustment of the weight vectors after all records have been matched. This is much like ‘epoch’ learning in supervised neural networks. The Batch-SOM is a more robust approach, since it mediated over a large number of learning steps. In this study, SOMs are generated by using Viscovery<sup>®</sup> SOMine 4.0 plus<sup>a</sup> produced by Eudaptics GmbH. In the SOMine, the uniqueness of the map is ensured by the adoption of the Batch-SOM and the linear initialization for input data. Much like some other SOMs<sup>28</sup>, SOMine creates a map in a two-dimensional hexagonal grid. Starting from numerical, multivariate data, the nodes on the grid gradually adapt to the intrinsic shape of the data distribution can be read off from the emerging map on the grid. The trained SOM is systematically converted into visual information<sup>23,29</sup>.

### III. Result

#### A. MDO Result

The population size was set on eight. It took roughly 20 hours of CPU time of JAXA’s super computer system 50 processing elements (PEs) for an Euler computation. Also, it took roughly five minutes of CPU time of one PE for a NASTRAN flutter computation. The total evolutionary computation of 18 generations was performed using 139 individuals, and 37 non-dominated solutions were obtained. The evolution might not converge yet. However, evolution was stopped because several non-dominated solutions was sufficient as the candidate of a compromise solution.

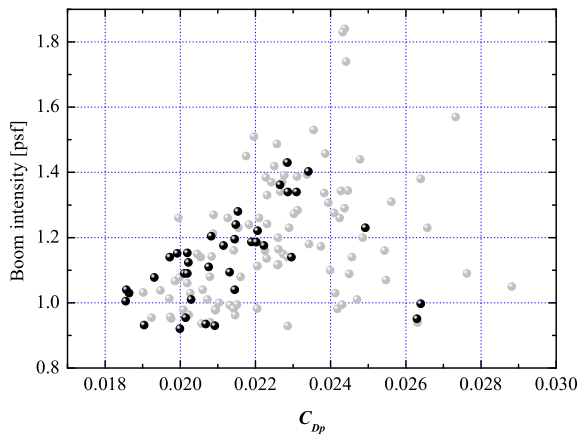
Figure 4 shows the all and derived non-dominated solutions projected on two-dimensional plane between two objectives. These plots indicates the following tradeoff information. There is no tradeoff between  $C_{Dp}$  and  $I_{boom}$  because the fuselage geometry, which obtains low boom and low drag performance, was fixed in the MDO.  $C_{Dp}$ ,  $I_{boom}$ , and  $W$  give similar effect on trim performance. When  $C_{Dp}$  is greater than roughly 0.0213, individual can trim independent on  $C_{Dp}$ . On the other hand, when  $C_{Dp}$  is lower than 0.0213, there is a tradeoff between them. When  $I_{boom}$  is greater than approximately 1.04, individual can similarly trim independent on  $I_{boom}$ . On the other hand, when  $I_{boom}$  is lower than 1.04, there is a tradeoff between them. Also, when  $W$  is greater than roughly 500, individual can trim independent on  $W$ . On the other hand, when  $W$  is lower than 500, there is a tradeoff between them. This fact indicates that there is no feasible tradeoff region in the present design space, because the trim performance gives tradeoffs for the other objective functions. The information which there is tradeoff between  $I_{boom}$  and trim performance is important for the design process, because the purpose of the S<sup>3</sup>TD is the demonstration of low-boom SST, and  $I_{boom}$  and trim performance should be better simultaneously for the practical design.

#### B. Data-Mining Result

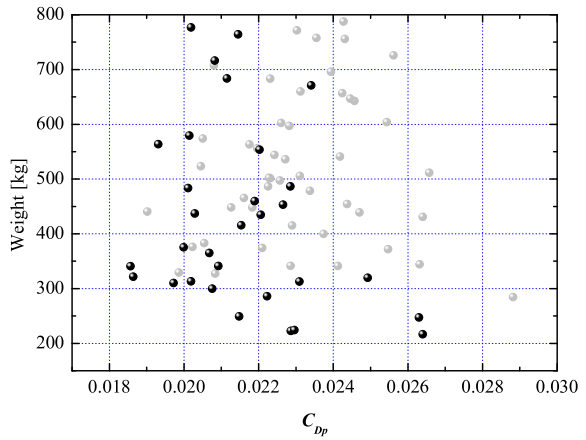
The data mining was performed for 37 non-dominated solutions to obtain the information to select the compromise solution. The acquired design information was presented to the designers of roughly 20 persons. It was employed as the resource of decision making to determine a compromise solution which was the prototype of S<sup>3</sup>TD 3rd configuration.

---

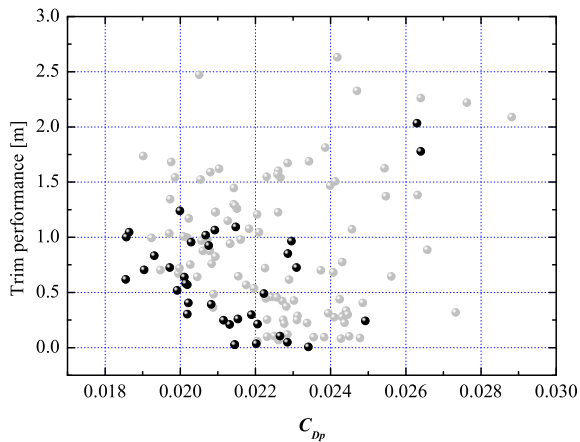
<sup>a</sup>“Eudaptics” available online at <http://www.eudaptics.com> [cited 5 June 2009].



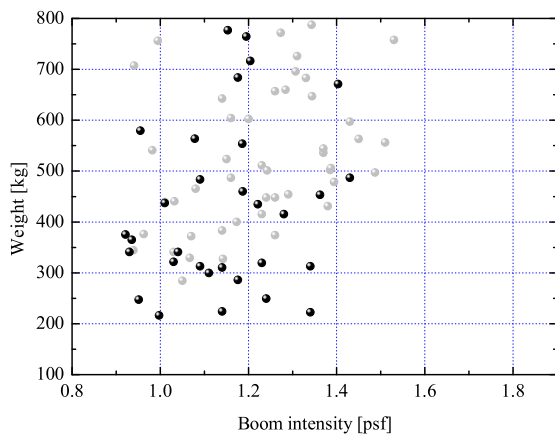
(a)  $C_{Dp}$  vs.  $I_{boom}$



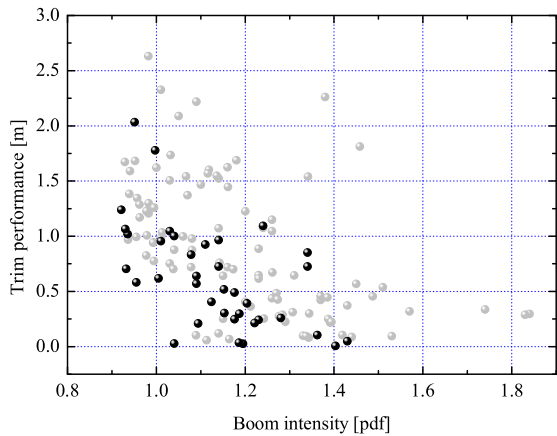
(b)  $C_{Dp}$  vs. Weight



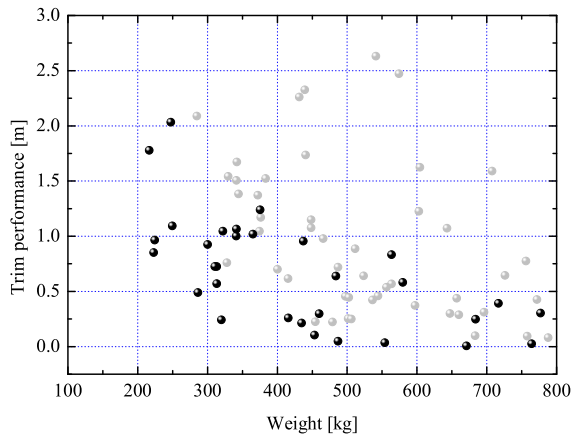
(c)  $C_{Dp}$  vs. Trim performance



(d)  $I_{boom}$  vs. Weight



(e)  $I_{boom}$  vs. Trim performance



(f) Weight vs. Trim performance

Figure 4. All and derived non-dominated solutions on two dimensional planes between the objective functions. The non-dominated solutions are plotted by using black color.

## 1. Knowledge Acquired by Using ANOVA

The variance of the design variables and their interactions by ANOVA are shown in Fig. 5. Their proportions are shown, which were larger than 1% to the total variance. In the present ANOVA analysis, as the input data is discontinuous, scant data is redeemed by using a kriging-based response surface. The information how the important design variable gives effect is insufficient on ANOVA. The aim of the ANOVA is to find out the important design variables.

Figure 5 (a) shows the effect proportion of the design variables for  $C_{Dp}$ . This figure reveals that the dv38 as the thickness in the vicinity of the leading edge at tip gives effect on  $C_{Dp}$ . Generally, when it becomes thick,  $C_{Dp}$  increases. When it becomes thin,  $C_{Dp}$  is decreased. Although the other wing thickness and leading-edge shape give effects on  $C_{Dp}$ , they does not have much effects because the perturbation is small in the 37 non-dominated solutions. That is, the only dv38 can re-design for the reduction of  $C_{Dp}$  to keep an individual as a non-dominated solution.

Figure 5 (b) shows the effect proportion of the design variables for the boom intensity. This figure reveals that dv22 and dv49 are important. The dv22 represents the curvature of the wing surface at the rear location of maximum thickness. When this curvature is low, the rear boom achieves low. The dv49 describes the twist angle at tip location. When this twist angle is large, as local angle of attack is negative, the front boom becomes large.

Two ANOVA works are performed for the structural weight. One case employs the database including six individuals not to fulfill the structural requirements. The other case uses the database eliminating the six individuals not to fulfill the structural requirements. The result of the first case is shown in Fig. 5 (c). This result shows the information of design variables to fulfill the structural requirements. The dv3 represents the angle of dihedral. This angle gives effect on the load distribution of the wing surface. The dv44 describes the maximum thickness position at tip. When this value is small, as the thickness near the trailing edge is thin, the strength cannot be maintained. The result of the second case is shown in Fig. 5 (d). This result shows the information of the design variables to reduce the structural weight(; besides structural requirements are fulfilled). The dv2 represents the angle of incidence of the wing. When this angle becomes large, the load distribution of the wing surface increases. The dv47 describes the twist angle at kink. This angle also gives similar effect on the load distribution of the wing surface. Although the wing thickness also gives effect on the structural weight, there is a constraint for the thickness to become non-dominated solution.

Figure 5 (e) shows the effect proportion of the design variables for the trim performance. The dv2 represents the angle of incidence of wing. As this angle gives effect on  $C_{Mp}$ , it is effective for the trim performance. The dv9 describes the curvature of the camber line near the leading edge at kink. When this design variable is large, as  $C_{Mp}$  increases, the body becomes instable. The dv50 represents the reflection angle of the stabilizer. This angle gives similar effect to dv2 and dv9. The dv47 describes the twist angle at kink. This angle also gives similar effect to dv2, dv9, and dv50. As the result of ANOVA is a surrogate model, the intimate effects indicated from the MDO results should be confirmed by using SOM.

## 2. Knowledge Acquired by Using SOM

The SOM is generated by using 37 non-dominated solutions to obtain the design knowledge to improve a compromise solution while it keeps the performance as a non-dominated solution. Figure 6 shows the generated SOM and colored maps by the four objective functions. The color pattern of them shows the tradeoffs among the four objects. The tradeoff information is summarized in Table 2. This result reveals that the trim performance is the important objective to determine the performances of the other objectives. That is, the present design space does not have the feasible tradeoff region. When the trim performance is improved, all of the other objectives becomes absolutely worse.

Figure 7 shows the color maps by the important design variables addressed by ANOVA. The effective design variables for  $C_{Dp}$  are dv38 and dv9. Figures 6 (b) and 7 (e) reveal that a large dv38 value increases  $C_{Dp}$ . A small dv38, however, does not improve  $C_{Dp}$  necessarily. Although there is no correlation between dv9 and  $C_{Dp}$  shown by the comparison between Figs. 6 (b) and 7 (c), dv9 should be small to become a non-dominated solution.

The effective design variables for  $I_{boom}$  are dv22 and dv49. The comparison between Figs. 6 (c) and 7 (d) reveals that a small dv22 reduces the boom intensity, though a large dv22 does not increase  $I_{boom}$ . Although there is no correlation between dv49 and  $I_{boom}$  shown by the comparison between Figs. 6 (c) and 7 (h), dv49 should be small to become a non-dominated solution.

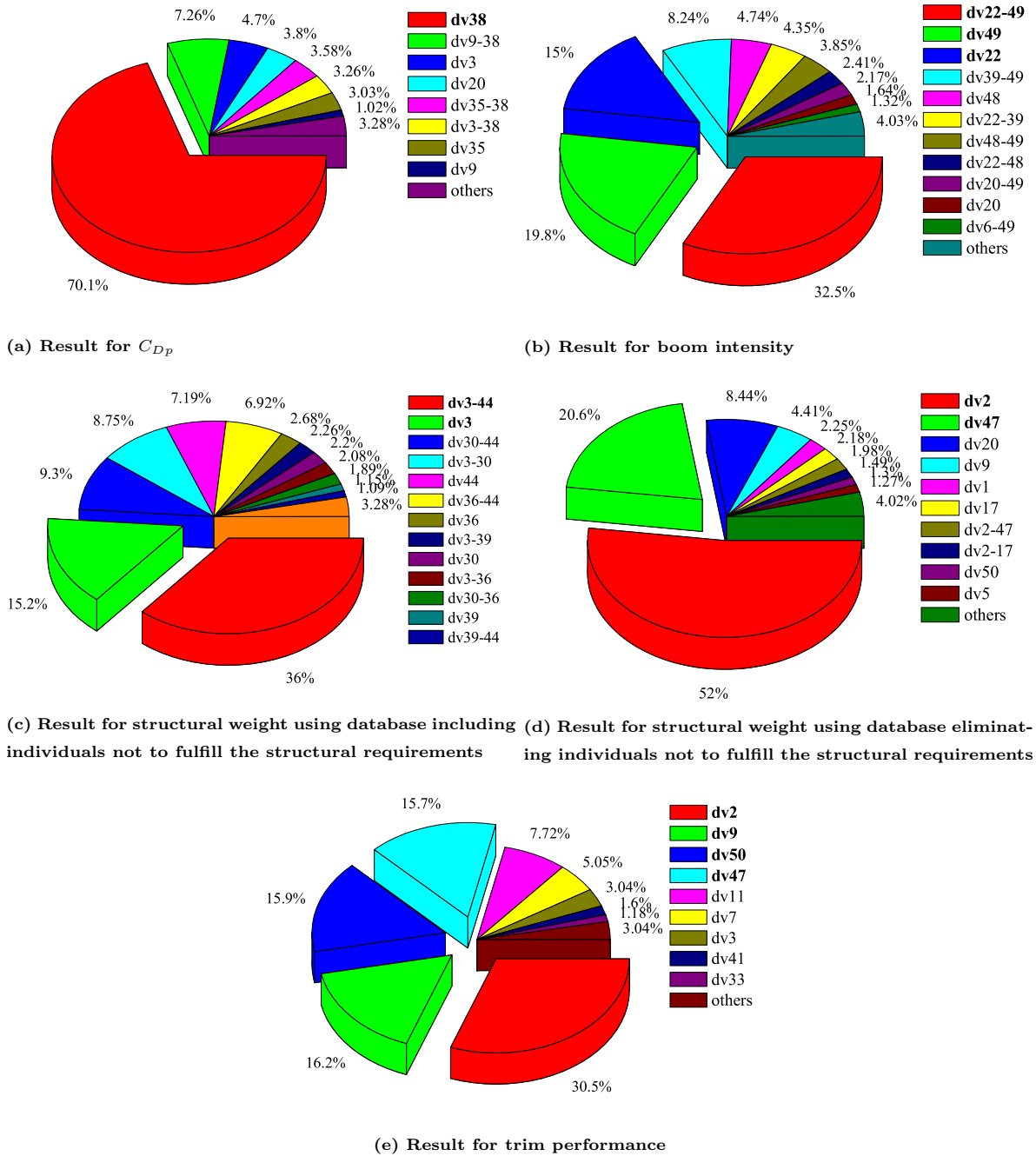


Figure 5. Proportion of design-variable influence for the objective functions using ANOVA.

**Table 2. Summarization of the tradeoff information among the four objective functions obtained by the color pattern on SOM.  $\circ$  denotes that there is tradeoff. On the other hand,  $\times$  means that there is no tradeoff.**

	$C_{D_p}$	$I_{boom}$	$W$	$ x_{cp} - x_{cg} $
$C_{D_p}$	\	$\times$	$\circ$	$\circ$
$I_{boom}$	—	\	$\times$	$\circ$
$W$	—	—	\	$\circ$
$ x_{cp} - x_{cg} $	—	—	—	\

**Table 3. The specification of the selected compromise solution.**

$C_{D_p}$	0.02092
$I_{boom}$	0.9301 [psf]
$W$	341.3 [kg]
$ x_{cp} - x_{cg} $	1.065 [m]
outboard wing	8plies $\times$ 4 sets
inboard wing	skin: 9.0 [mm], multi frames: 8.9 [mm]
design angle of attack	2.915 [deg]
reflection angle of stabilizer	-1.608 [deg]

The effective design variables for  $W$  are dv3 and dv44 when the all 37 solutions included the individuals not to fulfill the structural requirements consider. That is, the good design of dv3 and dv44 generates the solution to fulfill the structural requirements. The comparison between Figs. 6 (d) and 7 (b) reveals that a large dv3 improves the weight of the main wing, although a small dv3 increases the  $W$ . On the other hand, the comparison between Figs. 6 (d) and 7 (f) shows that a small dv44 improves the weight, although a large dv44 has no correction. The effective design variables for  $W$  are dv2 and dv47 when the solutions eliminated the individuals not to fulfill the structural requirements consider. The comparison between Figs. 6 (d) and 7 (a) reveals that a small dv2 improves the weight of the main wing, although a large dv2 increases the  $W$ . On the other hand, the comparison between Figs. 6 (d) and 7 (g) shows that a small dv47 improves the weight, although a large dv44 increases  $W$ .

The effective design variables for the trim performance are dv2, dv9, dv50, and dv47. The comparison between Figs. 6 (e) and 7 (a) reveals that a large dv2 improves the trim performance, although a small dv2 becomes the trim performance worse. The comparison between Figs. 6 (e) and 7 (c) reveals that a small dv2 is the necessary condition to improve the trim performance. The comparison between Figs. 6 (e) and 7 (i) reveals that a large dv50 becomes the trim performance worse. The comparison between Figs. 6 (e) and 7 (g) reveals that the large dv47 improves the trim performance, although a small dv47 becomes the trim performance worse.

Since there are tradeoffs between the trim performance and all of the other objective functions, the design variables as dv2, dv9, and dv50 effecting the trim performance determine the tradeoff among the objective functions. These design variables should be adequately designed to improve a compromise solution.

### C. Selection and Evaluation of Compromise Solution

The individual shown in Fig. 8 is selected using the information obtained by design-informatics approach. The concrete presented materials roughly classify into two groups. One is the information regarding the tradeoffs among the objective functions shown in Fig. 4. The SOM shown in Fig. 6 is also produced because it corroborates the tradeoffs. The other is the information concerning the candidates of a compromise solution. This includes the contour figure of  $C_p$  distribution at the supersonic cruising condition (like as Fig. 9), the specifications (as the objective-function values, number of laminations for composite material, thickness of aluminum material, the design angle of attack, and the reflection angle of the stabilizer), the

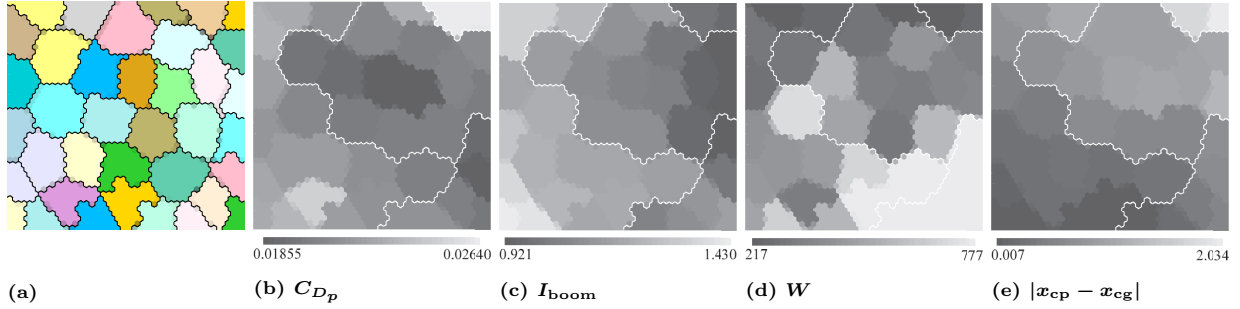


Figure 6. The resulting SOM separated by 37-non-dominated-solution region and SOMs colored by the objective functions.

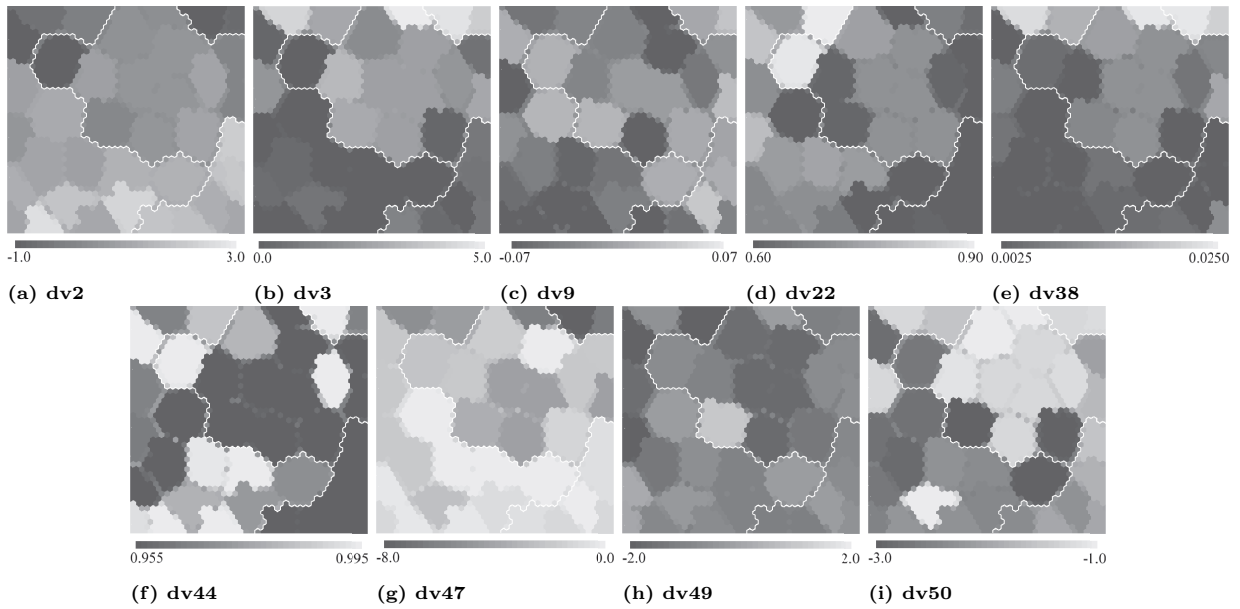


Figure 7. SOMs colored by the design variables which are indicated by ANOVA.

wing section and  $C_p$  distribution at root (21.62% spanwise location), kink (63.33%), and tip (99.00%) (like as Fig. 10), the spanwise  $C_L$ ,  $C_D$ , and twisting angle (like as Fig. 11), the ground pressure signature (like as Fig. 12), and the velocity-damping and velocity-frequency curves at each computational condition to seek the flutter speed (like as Fig. 13). Besides, the candidates are selected from the non-dominated solutions and individuals adjacent to them on Fig. 4(e), which indicates the relation between the boom intensity and the trim performance. The boom intensity has priority in this study. The trim performance gives tradeoffs for all of the other objective functions. The individual with disadvantageous manufacturing problem is excepted from the candidates. The important points are 1) the performance of all objective functions and 2) the possibility for the improvement of the other three objectives to keep the boom performance. On the final decision of a compromise solution, the individual which the wing section to be alike NEXST-1 was selected. That is, the shape of the selected compromise solution convinces regarding aerodynamics and manufacture. It is shown in Fig. 8. The trim performance was concluded to be improved by the regulation of the reflection angle of stabilizer (the outside range set in the present optimization is namely reconsidered). Therefore, a weak non-dominated solution was ventured to select for a compromise solution.

Table 3 shows the specification of the compromise solution. It is notable that the criteria of the design angle of attack and the reflection angle of stabilizer is the horizontal line (longitudinal axis of body) for three views. Thus, the reflection angle is defined for longitudinal axis of body and is independent of angle of attack. This result shows that the trim performance is insufficient. The results from ANOVA shown in Fig. 5 indicate that the cant angle (dv2) and the geometry (dv9 and dv47) of the main wing which are influent in the trim performance give effects on several objective function. However, the reflection angle of the stabilizer does not give effect on any objective functions except the trim performance. Since the designed reflection angle of the stabilizer can afford to be harder, the modification of it can improve the trim performance.

Figure 9 shows the  $C_p$  distributions on upper surface and on symmetrical plane. This figure reveals that the shock waves occur around the front location of the engine and bumps into the upper surface of the main wing. Although the shock wave is shielded, the performance of the wing is down. It is important to design the geometry of the wing for the alleviation of this shock wave.

Figure 10 shows the  $C_p$  distributions and the wing sections at root, kink, and tip location. At the root location, since two shock waves bump into the wing upper surface, the increase of the wing thickness obtains insufficient lift performance and augment the induced drag. On the other hand, it reveals the connection between the structural weight and the structural requirements. The constraint of the thickness at root is  $5\% \pm 1\%$  chord length. The thickness of the compromise solution at root is 4.4% chord length. The thickness of the compromise solution becomes thin with the fulfillment of the structure requirements. At the kink location, upper surface near leading edge dents, because this depression moderates the shock wave occurred from the front of the engine. This hollow is the key to improve the aerodynamic performance. The maximum thickness at kink is 5.4% chord length. The thickness at kink location should be simultaneously thick to have sufficient aerodynamic performance and to fulfill the structural requirements. At the tip location, the wing has insufficient aerodynamic performance as shown in Fig. 11. Since the wing geometry in the vicinity of the tip gives strict effects on the boom intensity indicated by the data-mining results, the wing tip geometry is evolved to reduce the boom intensity. In addition, the strong shock wave occurs around the rear part of the fuselage. As this corrupts the rear boom intensity, the re-consideration is needed.

Figure 12 shows the ground pressure signatures of the compromise solution. The wide line represented in this figure is the signature which gives  $[|\Delta P_{\max}| + |\Delta P_{\min}|]_{\max} (I_{\text{boom,max}})$ . This figure indicates that the both peaks of the front and rear boom intensity are weakened because of no simple N-wave. The data mining reveals that three design variables for the main wing such as the cant angle for attachment to fuselage, twisting angle, and the bluntness of the leading edge give effects on the front boom. It similarly reveals that the design variable as the reflection angle of stabilizer gives effect on the rear boom. Especially, the inboard wing with camber on the trailing edge improves the rear boom intensity. Because, the strong expansion wave from the trailing edge extinguishes the positive pressure from the lifting surface of the rear fuselage. Moreover, the large negative reflection angle of the stabilizer causes the strong rear boom intensity due to the similar reason. But, the negative reflection angle is necessary to trim. The reflection angle of the stabilizer is essential in the present design problem.

Figure 13 shows the velocity-damping and velocity-frequency curves of the four computational Mach-number conditions. Each mode corresponds to the following; mode1 with the bending 1st mode, mode2 with the twisting 1st mode, mode3 with the bending 2nd mode, and mode4 with the twisting 2nd mode. It reveals that the twisting 2nd mode decides the flutter speeds at all of the Mach-number conditions, and

their speeds are roughly 700m/sEAS. It is occurred by the coupling flutter between the twisting 1st and 2nd modes. Therefore, the compromise solution has the competent margin for the wing flutter limitation. In this study, as the flutter only for the main wing is considered, the occurring number of modes is small. The actual flutter speed anticipates to be occurred by the couple between the mode at wing and one at fuselage. In the design phase, the detailed flutter characteristic would be investigated.

## IV. Conclusion

The design-informatics approach has been proposed for the efficient design, in which the construction of the design database is implemented and the design information is extracted from it. This information systematizes the design space, and assists the efficient selection of a compromise solution. In the present study, the approach has been applied to the intimate configuration of the silent supersonic technology demonstrator projected by Japan Aerospace Exploration Agency for the conceptual design of the 3rd configuration of the silent supersonic technology demonstrator under the design requirements among the aerodynamic, sonic-boom, structural, and trim performances. The process of the approach gave the tradeoffs among the defined design requirements, namely objective functions. Thereby, it was revealed that the improvement of the trim performance corrupts the other requirements. Furthermore, the important design variables were evident, and the correlations between the design requirements and them were also shown. The obtained design information was produced to the designers and it was employed as the resource of decision making to determine a compromise solution. The knowledge was produced for the future design. The design-informatics approach is an efficient and effective design manner, and moreover an innovative and creative design can be pursued.

## Acknowledgments

We would first like to thank all members of the supersonic transport team in aviation program group, JAXA for providing useful advice. The Euler/NASTRAN computations were performed by using the CeNSS of Numerical Simulator III in JAXA's engineering digital innovation(JEDI) center, JAXA. We would also like to thank Ms. Masako Tsuchiya and Mr. Masahiro Yoshida, the managers in JEDI center, for their kind help regarding the CeNSS employment. In addition, the technical comment from Dr. Kouji Shimoyama regarding the self-organizing map is also sincerely acknowledged.

## References

- <sup>1</sup>Murakami, A., "Silent Supersonic Technology Demonstration Program," *Proceedings on 25th International Council of the Aeronautical Sciences*, ICAS 2006-1.4.2, Hamburg, Germany, 2006.
- <sup>2</sup>Ohnuki, T., Hirako, K., and Sakata, K., "National Experimental Supersonic Transport Project," *Proceedings on 25th International Council of the Aeronautical Sciences*, ICAS 2006-1.4.1, Hamburg, Germany, 2006.
- <sup>3</sup>Chiba, K., Makino, Y., and Takatoya, T., "Evolutionary-Based Multidisciplinary Design Exploration for Silent Supersonic Technology Demonstrator Wing," *Journal of Aircraft*, Vol. 45, No. 5, 2008, pp. 1481-1494.
- <sup>4</sup>Jeong, S., Hasegawa, S., Shimoyama, K., and Obayashi, S., "Development and Investigation of Efficient GA/PSO-Hybrid Algorithm Applicable to Real-World Design Optimization," *IEEE Computational Intelligence Magazine*, August 2009, pp. 36-44.
- <sup>5</sup>Chiba, K. and Obayashi, S., "Knowledge Discovery in Aerodynamic Design Space for Flyback-Booster Wing Using Data Mining," *Journal of Spacecraft and Rockets*, Vol. 45, No. 5, 2008, pp. 975-987.
- <sup>6</sup>Kennedy, J. and Eberhart, R., "Particle Swarm Optimization," *Proceedings of the Fourth IEEE International Conference on Neural Networks*, 1995, pp. 1942-1948.
- <sup>7</sup>Alvarez-Benitez, J. E., Everson, R. M., and Fieldsend, J. E., "A MOPSO Algorithm Based Exclusively on Pareto Dominance Concepts," *The 3rd International Conference on Evolutionary Multi-Criterion Optimization, LNCS 3410*, Springer-Verlag Heidelberg, Guanajuato, Mexico, 2005, pp. 459-473.
- <sup>8</sup>Fonseca, C. M. and Fleming, P. J., "Genetic Algorithms for Multiobjective Optimization: Formulation, Discussion and Generalization," *Proceedings of the Fifth International Conference on Genetic Algorithms*, 1993, pp. 416-423.
- <sup>9</sup>Obayashi, S., Takahashi, S., and Takeguchi, Y., "Niching and Elitist Models for MOGAs, Parallel Problem Solving from Nature," *The 5th International Conference on Parallel Problem Solving from Nature, LNCS 1498*, Springer, Berlin, Heidelberg, New York, 1998, pp. 260-269.
- <sup>10</sup>Simpson, T. W., Mauery, T. M., Korte, J. J., and Mistree, F., "Kriging Models for Global Approximation in Simulation-Based Multidisciplinary Design Optimization," *AIAA Journal*, Vol. 39, No. 12, 2001, pp. 2233-2241.
- <sup>11</sup>Keane, A. J., "Statistical Improvement Criteria for Use in Multiobjective Design Optimization," *AIAA Journal*, Vol. 44, No. 4, 2006, pp. 879-891.

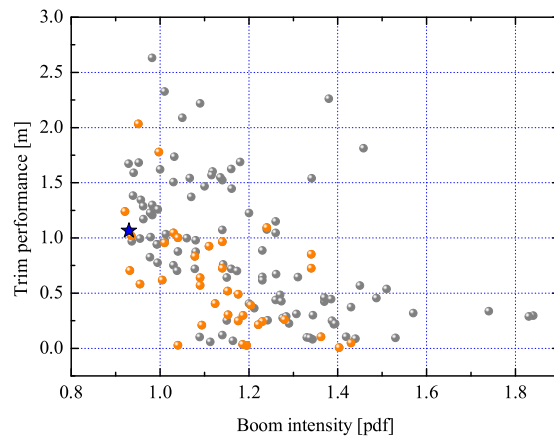


Figure 8. Location of compromise solution projected onto two dimensional plots between boom intensity and trim performance. The star plot denotes the selected compromise solution.

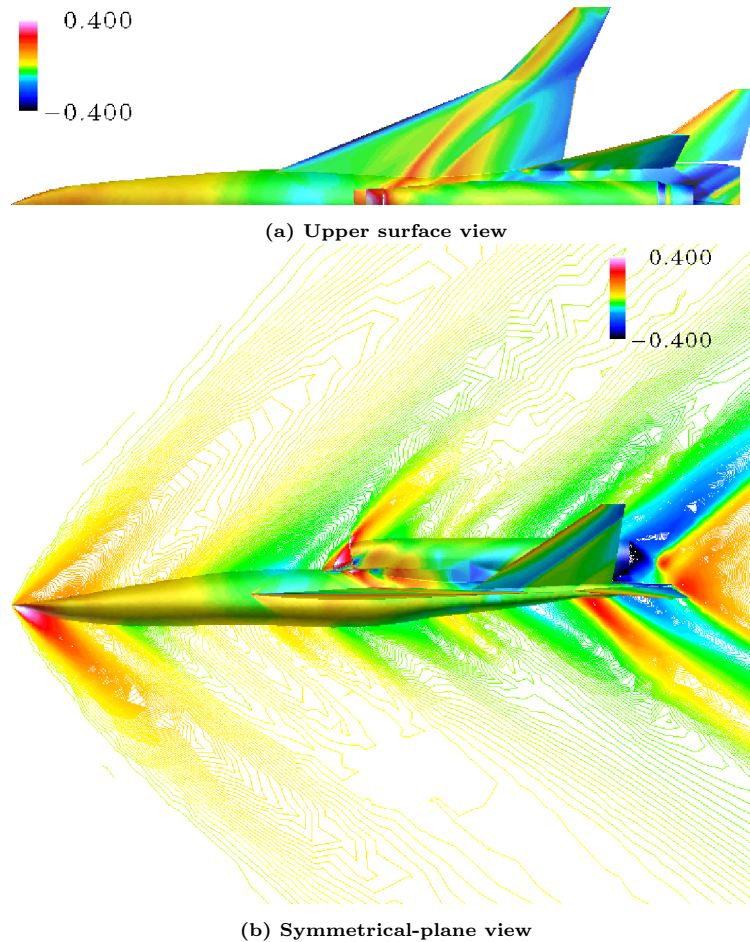
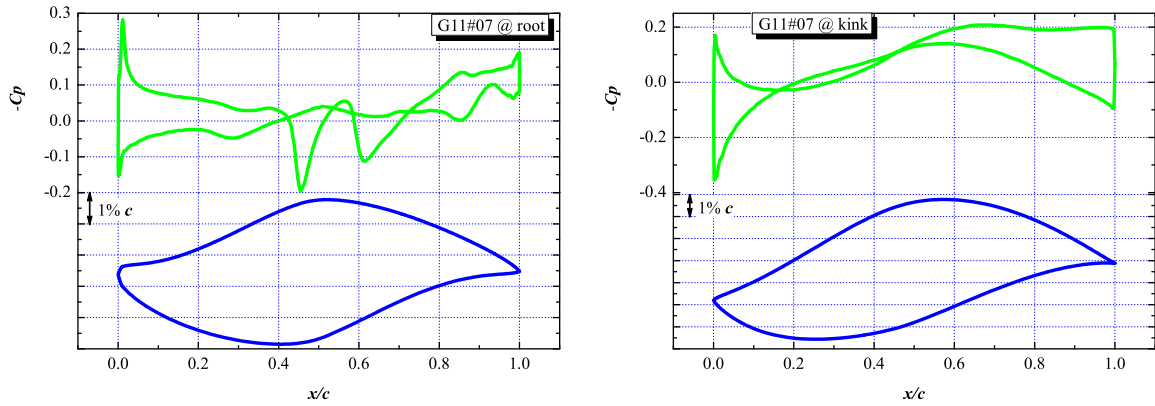
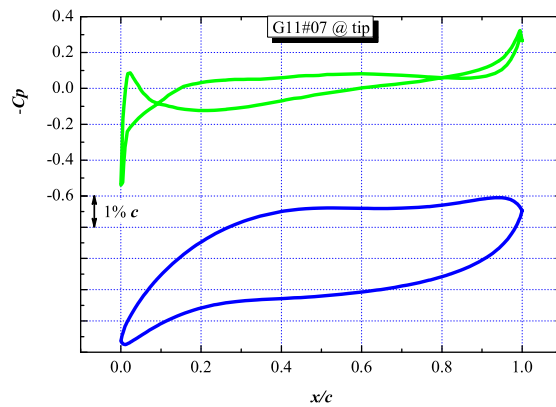


Figure 9.  $C_p$  distribution of the decided compromise solution. The angle of attack of 2.915deg is set to achieve the target  $C_L$ .



(a) Airfoil shape at root (21.62% spanwise location)      (b) Airfoil shape at kink (63.33% spanwise location)



(c) Airfoil shape at tip (99.00% spanwise location)

Figure 10. The characteristic values of the decided compromised solution.

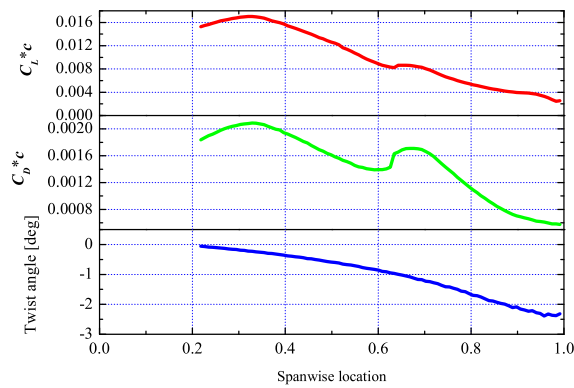
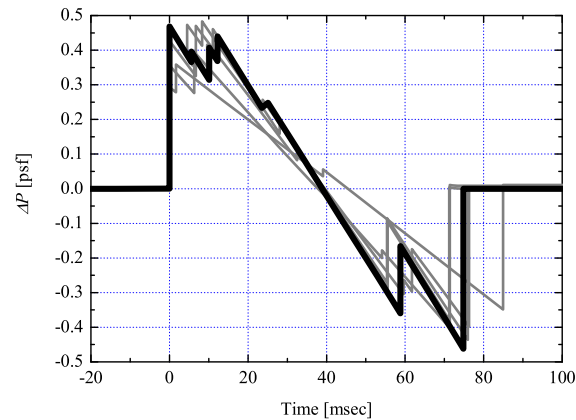


Figure 11. Spanwise distributions of  $C_L$ ,  $C_{Dp}$ , and twist angle for the compromise solution.



**Figure 12.** The ground pressure signatures of the compromise solution. The bold line shows the signature with the maximum value of  $I_{boom}$ .

<sup>12</sup>Jeong, S., Murayama, M., and Yamamoto, K., “Efficient Optimization Design Method Using Kriging Model,” *Journal of Aircraft*, Vol. 42, No. 2, 2005, pp. 413–420.

<sup>13</sup>Keane, A. J., “Wing Optimization Using Design of Experiment, Response Surface, and Data Fusion Methods,” *Journal of Aircraft*, Vol. 40, No. 4, 2003, pp. 741–750.

<sup>14</sup>Eshelman, L. J. and Schaffer, J. D., “Real-Coded Genetic Algorithms and Interval Schemata,” *Foundations of Genetic Algorithms 2*, Morgan Kaufmann, San Mateo, CA, 1993, pp. 187–202.

<sup>15</sup>Takahashi, M. and Kita, H., “A Crossover Operator Using Independent Component Analysis for Real-Coded Genetic Algorithms,” *Proceedings of IEEE Congress on Evolutionary Computation 2001*, 2001, pp. 643–649.

<sup>16</sup>Umeda, M., Takenaka, K., Hatanaka, K., Hirayama, D., Yamazaki, W., Matsushima, K., and Nakahashi, K., “Validation of CFD Capability for Supersonic Transport Analysis Using NEXST-1 Flight Test Results,” AIAA Paper 2007-4437, 2007.

<sup>17</sup>Kawakami, H., Takatoya, T., and Ishikawa, H., “Static Aeroelastic Analysis of Supersonic Experimental Airplane NEXST-1 Flight Test,” AIAA Paper 2007-4174, 2007.

<sup>18</sup>Makino, Y. and Naka, Y., “Sonic-Boom Research and Low-Boom Demonstrator Project in JAXA,” *Proceedings on 19th International Congress on Acoustics*, NLA-08-002-IP, Madrid, Spain, 2007.

<sup>19</sup>Ito, Y. and Nakahashi, K., “Direct Surface Triangulation Using Stereolithography Data,” *AIAA Journal*, Vol. 40, No. 3, 2002, pp. 490–496.

<sup>20</sup>Obayashi, S. and Guruswamy, G. P., “Convergence Acceleration of an Aeroelastic Navier-Stokes Solver,” *AIAA Journal*, Vol. 33, No. 6, 1994, pp. 1134–1141.

<sup>21</sup>Venkatakrishnan, V., “On the Accuracy of Limiters and Convergence to Steady State Solutions,” AIAA Paper 93-0880, 1993.

<sup>22</sup>Sharov, D. and Nakahashi, K., “Reordering of Hybrid Unstructured Grids for Lower-Upper Symmetric Gauss-Seidel Computations,” *AIAA Journal*, Vol. 36, No. 3, 1998, pp. 484–486.

<sup>23</sup>Obayashi, S. and Sasaki, D., “Visualization and Data Mining of Pareto Solutions Using Self-Organizing Map,” *The 2nd International Conference on Evolutionary Multi-Criterion Optimization, LNCS 2632*, Springer-Verlag Heidelberg, Faro, Portugal, 2003, pp. 796–809.

<sup>24</sup>Holden, C. M. E. and Keane, A. J., “Visualization Methodologies in Aircraft Design,” AIAA Paper 2004-4449, 2004.

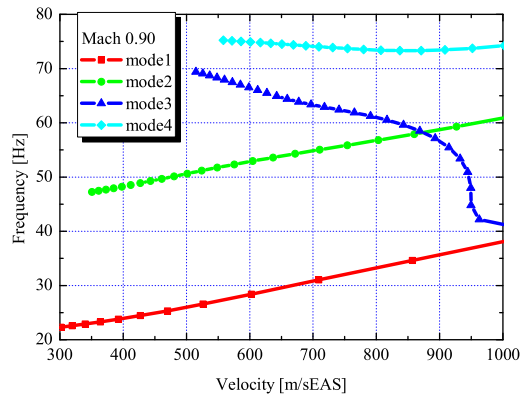
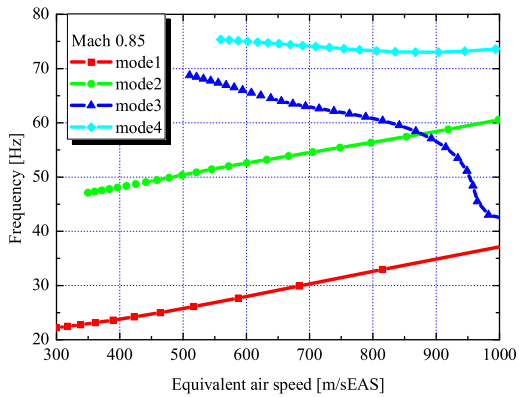
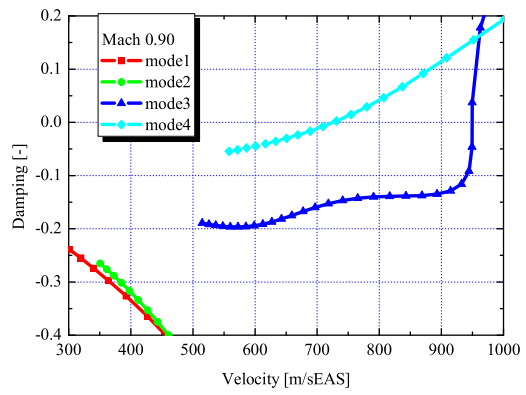
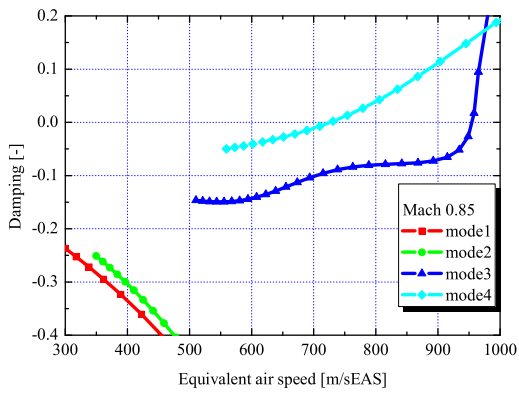
<sup>25</sup>Sobol, I. M., “Sensitivity Estimates for Nonlinear Mathematical Models,” *Mathematical Modelling and Computational Experiments*, Vol. 1, No. 4, 1993, pp. 407–414.

<sup>26</sup>Jones, D. R., Schonlau, M., and Welch, W. J., “Efficient Global Optimization of Expensive Black-Box Functions,” *Journal of Global Optimization*, Vol. 13, No. 4, 1998, pp. 455–492.

<sup>27</sup>Kohonen, T., *Self-Organizing Maps*, Springer, Berlin, Heidelberg, 1995.

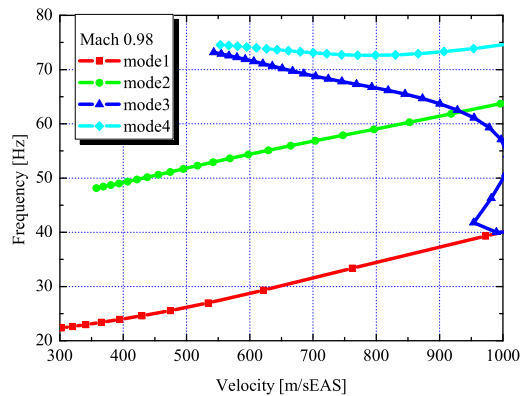
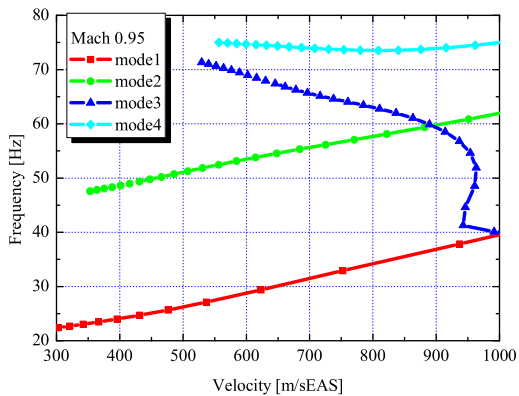
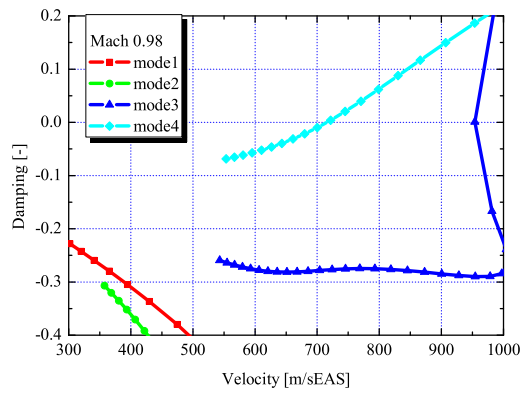
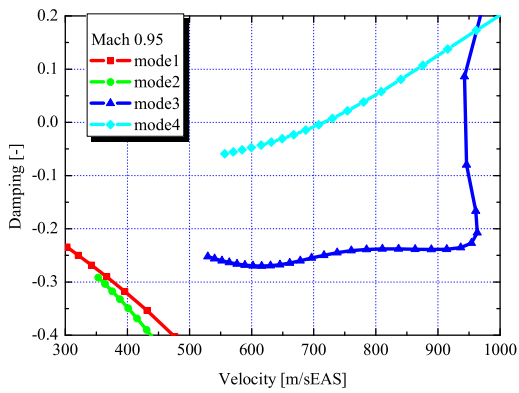
<sup>28</sup>Vesanto, J. and Alhoniemi, E., “Clustering of the Self-Organizing Map,” *IEEE Transactions on Neural Networks*, Vol. 11, No. 3, 2000, pp. 586–600.

<sup>29</sup>Chiba, K., Oyama, A., Obayashi, S., Nakahashi, K., and Morino, H., “Multidisciplinary Design Optimization and Data Mining for Transonic Regional-Jet Wing,” *Journal of Aircraft*, Vol. 44, No. 4, 2007, pp. 1100–1112.



a) Mach 0.85

b) Mach 0.90



c) Mach 0.95

d) Mach 0.98

Figure 13. V-g and V-f plots of the decided compromise solution.